

Non-destructive search for interstellar dust using synchrotron microprobes

A. J. Westphal¹, A. Allbrink^{2*}, C. Allen³, S. Bajt⁴, R. Bastien³, H. Bechtel⁵, P. Bleuet⁶, J. Borg⁷, S. Bowker^{8*}, F. Brenker⁹, J. Bridges¹⁰, D. E. Brownlee¹¹, M. Burchell¹², M. Burghammer⁶, A. L. Butterworth¹, A. Campanile^{13*}, P. Cloetens⁶, G. Cody¹⁴, T. Ferroir¹⁵, K. Ferrari^{16*}, C. Floss¹⁷, G. J. Flynn¹⁸, D. Frank³, Z. Gainsforth¹, E. Grün¹⁹, M. Harmer^{20*}, P. Hoppe²¹, A. Kearsley²², S. Kulkarni^{23*}, B. Lai²⁴, L. Lemelle¹⁵, H. Leroux²⁵, R. Lettieri¹, W. Marchant¹, B. McCreadie^{26*}, L. R. Nittler¹⁴, R. Ogliore¹, F. Postberg¹⁹, C. Rigamonti^{27*}, S. A. Sandford²⁸, S. Schmitz⁹, G. Silversmit²⁹, A. Simionovici³⁰, G. Sperry^{31*}, R. Srama¹⁹, F. Stadermann¹⁹, T. Stephan³², R. M. Stroud³³, J. Susini⁶, S. Sutton²⁴, V. Thompson^{34*}, R. Toucoulou⁶, M. Trieloff¹⁹, P. Tsou¹⁶, A. Tsuchiyama³⁵, T. Tyliczszak⁵, B. Vekemans²⁹, L. Vincze²⁹, J. Warren³, T. Yahnke^{37*}, D. Zevin¹, M. E. Zolensky³, >27,000 Stardust@home dusters^{38*}

¹Space Sciences Laboratory, U. C. Berkeley, USA, ²Rhede, Germany, ³KT NASA Johnson Space Center, USA, ⁴DESY, Hamburg, Germany, ⁵Advanced Light Source, Lawrence Berkeley Laboratory, USA, ⁶European Synchrotron Radiation Facility, Grenoble, France, ⁷IAS Orsay, France, ⁸Chatman, Kent, UK, ⁹Geoscience Institute, Universität Frankfurt am Main, Frankfurt, Germany, ¹⁰Space Research Centre, University of Leicester, Leicester, UK, ¹¹Astronomy Dept., University of Washington, USA, ¹²University of Kent, UK, ¹³Reggio Emilia, Italy, ¹⁴Carnegie Institution of Washington, USA, ¹⁵ENS, Lyon, France, ¹⁶Jet Propulsion Laboratory, USA, ¹⁷Physics Dept., Washington University, USA, ¹⁸Dept. of Physics, SUNY – Plattsburgh, USA, ¹⁹Max-Planck-Institut für Kernphysik, Heidelberg, Germany, ²⁰Beverley, East Yorkshire, UK, ²¹Max-Planck-Institut für Chemie, Germany, ²²IARC, Dept. of Mineralogy, The Natural History Museum, UK, ²³Pune, Maharashtra, India, ²⁴Advanced Photon Source, Argonne National Laboratory, USA, ²⁵Université des Sciences et Technologies de Lille, France, ²⁶Downingtown, Pennsylvania, USA, ²⁷Moncalieri, Torino, Italy, ²⁸Astrophysics Branch, NASA-Ames Research Center, USA, ²⁹University of Ghent, Belgium, ³⁰Observatoire des Sciences de l'Univers de Grenoble, France, ³¹Tacoma, Washington, USA, ³²University of Chicago, USA, ³³Naval Research Laboratory, Washington DC, USA, ³⁴Eugene, Oregon, USA, ³⁵Osaka University, Japan, ³⁶Institut für Geowissenschaften, University of Heidelberg, Germany, ³⁷St. Louis, Missouri, USA, ³⁸Worldwide
* Stardust@home duster

Abstract. Here we describe the critical role that synchrotron X-ray and infrared microprobes are playing in the search for interstellar dust in the Stardust Interstellar Dust Collector (SIDC). The samples under examination are submicron particles trapped in low-density aerogel. We have found that the spatial resolution, energy range, and flux capabilities of the FTIR beamlines 1.4.3, ALS, and U2B, NSLS; the XRF microprobes ID13 and ID22NI, ESRF and 2-ID-D, APS; and the STXM beamline 11.0.2, ALS are ideally suited for studying these tiny returned samples. Using nondestructive, coordinated analyses at these microprobes, we have been able to eliminate most candidates as likely samples of interstellar dust. This in itself is a major accomplishment, since the analysis of these tiny samples is technically extremely challenging.

Keywords: Interstellar dust, stardust

PACS: 96.30.Vb Dust, extraterrestrial materials

INTRODUCTION

The Stardust cometary and interstellar dust sample return mission was launched by NASA in 1999. Stardust

was the first sample return mission to deliver solid samples from beyond the Moon. It exposed a ~ 0.1 m² collector consisting of aerogel tiles and strips of aluminum foil to the interstellar dust stream for 195 days during

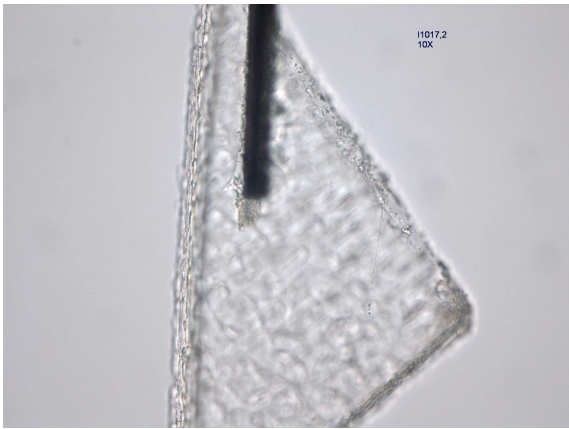


FIGURE 1. Off-normal track I1017,2 in an aerogel keystone. The track is 300 μm long and 2.5 μm in diameter.

two collection periods in 2000 and 2002 [1]. In January 2004, it collected cometary dust from the coma of comet 81P/Wild 2 in a similar but distinct collector, and both collectors were returned in January 2006. Synchrotron X-ray and infrared microprobes have played a critical role in the analysis of samples of cometary dust returned by Stardust [2, 3, 4, 5, 6]. Here we describe the critical role that synchrotron microprobes are now playing in the search for interstellar dust in the Stardust Interstellar Dust Collector.

EXPECTED PROPERTIES OF INTERSTELLAR DUST

Interstellar dust, entering in a direction approximately opposite to the direction of the Sun's motion through the local interstellar medium, was detected in our Solar System by the Galileo and Ulysses spacecraft [7]. The spacecraft observations indicate that ~ 30 interstellar particles mostly from 0.3 to 0.6 μm in size, much smaller than the comet particles that were previously analyzed, should have impacted that 0.1 m^2 collector. The mineralogy of interstellar dust is inferred from astronomical infrared spectroscopy, which detects vibrational, stretching, and bending modes of the molecules in solids, and from laboratory studies of isotopically anomalous presolar grains in meteorites. The two dominant solids in the interstellar medium are believed to be amorphous silicates, with the ratio of crystalline to amorphous silicates being $<4\%$, and organic matter. For the refractory elements the elemental composition of the interstellar dust is inferred by subtracting the composition of the gas phase, determined by spectroscopy, from the presumed starting composition [8]. The inferred average interstellar dust composition is similar to that of the primitive CI class of meteorites. But

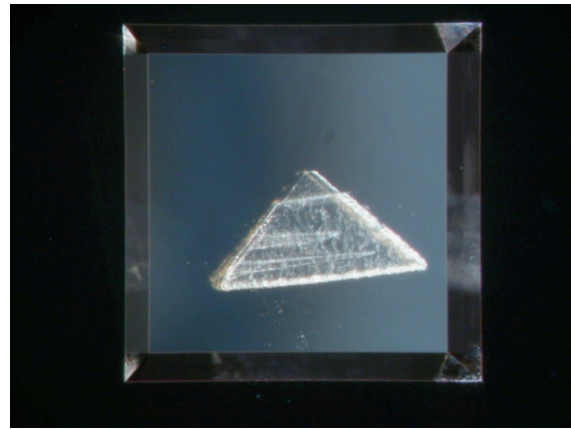


FIGURE 2. Picokeystone in a Si_3N_4 sandwich. The window is 1.5mm square.

the moderately-volatile elements, such as S, Cu and Zn, are not significantly depleted in the gas phase, so they are expected to be underabundant in the dust compared to the CI composition. The composition and mineralogy are expected to provide clues to distinguish interstellar dust from spacecraft debris, although the properties inferred from remote sensing are only average values over a large number of grains. The relatively high uncertainties in chemical composition and abundance of different dust species may also be constrained by theoretical considerations of dust production and processing in the ISM [9].

CANDIDATE IDENTIFICATION AND SAMPLE PREPARATION

The first challenge is to locate the interstellar impacts, with only ~ 30 impacts in 0.1 m^2 of aerogel. Approximately 36% of the aerogel tiles in the SIDC have been digitally imaged with $\sim 0.5 \mu\text{m}$ resolution using an automated microscope. The digital imagery consists of stacks of ~ 40 images in each field of view of the microscope, spanning $\sim 200 \mu\text{m}$ in focus range. Volunteer citizen scientists ("dusters") search the images for candidate impacts using a web-based virtual microscope to focus through the image stacks in each field of view. To qualify to participate, the volunteers must take web-based training and pass a test. More than 27,000 volunteers have qualified to participate. Such an unusual approach requires careful quantitative evaluation. The detection efficiency and false positive rate ("sensitivity" and "specificity", respectively) are measured for all dusters using fields of view in which images of impacts from laboratory simulations have been dubbed, or images which have already been examined and are assessed to be blank

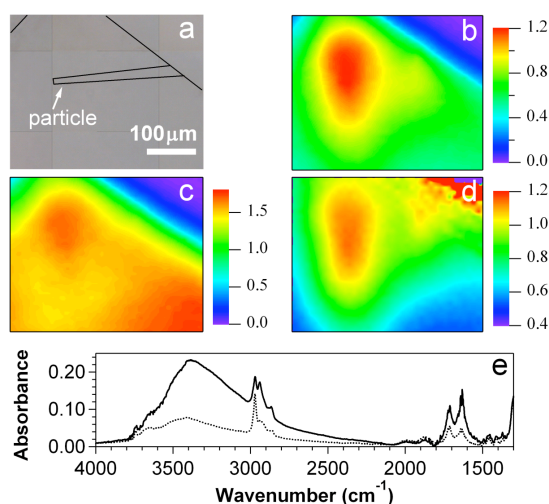


FIGURE 3. FTIR analysis of off-normal track I1017,2,1,0,0 at beamline 1.4.3 at the ALS. (a) Optical image showing the edges of keystone and the terminal particle. The entrance of the particle into the aerogel is from the right side. (b) Absorbance area map for the CH₂ feature at 2940 cm⁻¹. (c) Absorbance area map for the CH₃ feature at 2970 cm⁻¹. (d) Absorbance peak height map for the CH₃ feature at 2970 cm⁻¹. The dimensional scale bar is the same for (a), (b), (c), and (d) and the false color image scale for (b), (c), and (d) are in absorbance units. (e) IR spectra from the terminal particle (red trace) and from a “clean” aerogel area (black trace) located far from the track.

by the Stardust@home team at Berkeley. The images of the impacts are scaled to allow a measurement of sensitivity as a function of track diameter and depth. The average individual sensitivity is >90% for tracks > 5 μm in diameter, which corresponds to an impactor diameter of ~ 500 nm assuming the empirical scaling of Burchell et al. [10]. Through Stardust@home, we have identified 29 *bona fide* high-angle tracks in the collector. Some of these projectiles are consistent with secondary ejecta originating from three separate impacts on the spacecraft, but some have a trajectory that is consistent with the interstellar dust stream, and may be interstellar dust impacts. The tracks are < 3 μm in diameter; these provide an independent validation of the Stardust@home approach. Approximately 100 candidates have been identified in the 247 cm² searched area, through duster response data plus verification by the Stardust@home team and a “Red Team” recruited from the top dusters. Since only ~30 interstellar grains are expected to have hit the entire collector, we expect to have to characterize ~12 candidates, on average, to find a single interstellar impact. In order to verify the extraction and analysis techniques, the first candidates that we examined were particles whose directions suggested they were likely debris from the spacecraft, rather than the rare interstellar parti-

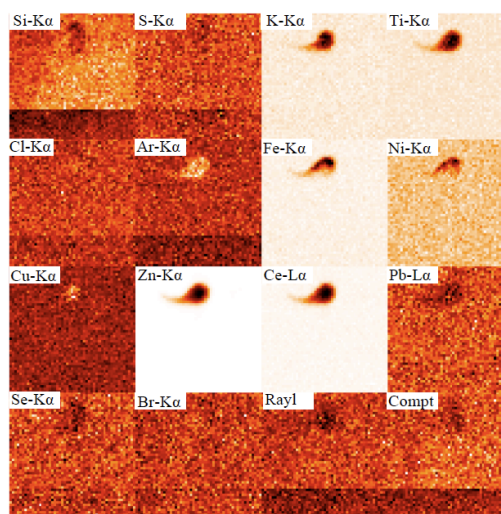


FIGURE 4. XRF maps of terminal particle in track I1017,2 taken at beamline ID13 at ESRF. The scan region is 10 μm × 10 μm in size.

cles.

We extracted the impact candidates from the interstellar collector in so-called “picokeystones” [11] — these are wedge-shaped volumes of aerogel machined from the tiles using glass needles controlled by automated micro-manipulators. The candidates are located in a thin (50 – 70 μm) section of the picokeystone (Figure 2) so that all synchrotron-based analytical techniques can be applied. The picokeystones are extracted on barbed polysilicon forks, then carefully transferred to a sandwich consisting of two 70 nm-thick Si₃N₄ windows (Figure 2). This mounting technique simultaneously protects the samples from contamination, reduces risk of loss by physically trapping the samples, and allows for all synchrotron-based analyses except tomography, which has a reduced resolution due to limitations in the angular scan range.

FTIR SCREENING FOR ORGANICS

Before X-ray microprobe analysis, interstellar grain candidates were examined by Fourier Transform Infrared Spectroscopy on beamline 1.4.3 at the Advanced Light Source, Lawrence Berkeley Laboratory and at beamline U2B at the National Synchrotron Light Source at Brookhaven National Laboratory. Scans were done with diffraction-limited beams. We have found that the native organics in the aerogel picokeystones are highly variable both in concentration and in species. We have also found that synchrotron X-ray analysis induces a change in the organic concentration and speciation. This effect can be quantified and will be important in establishing X-ray dose limits.

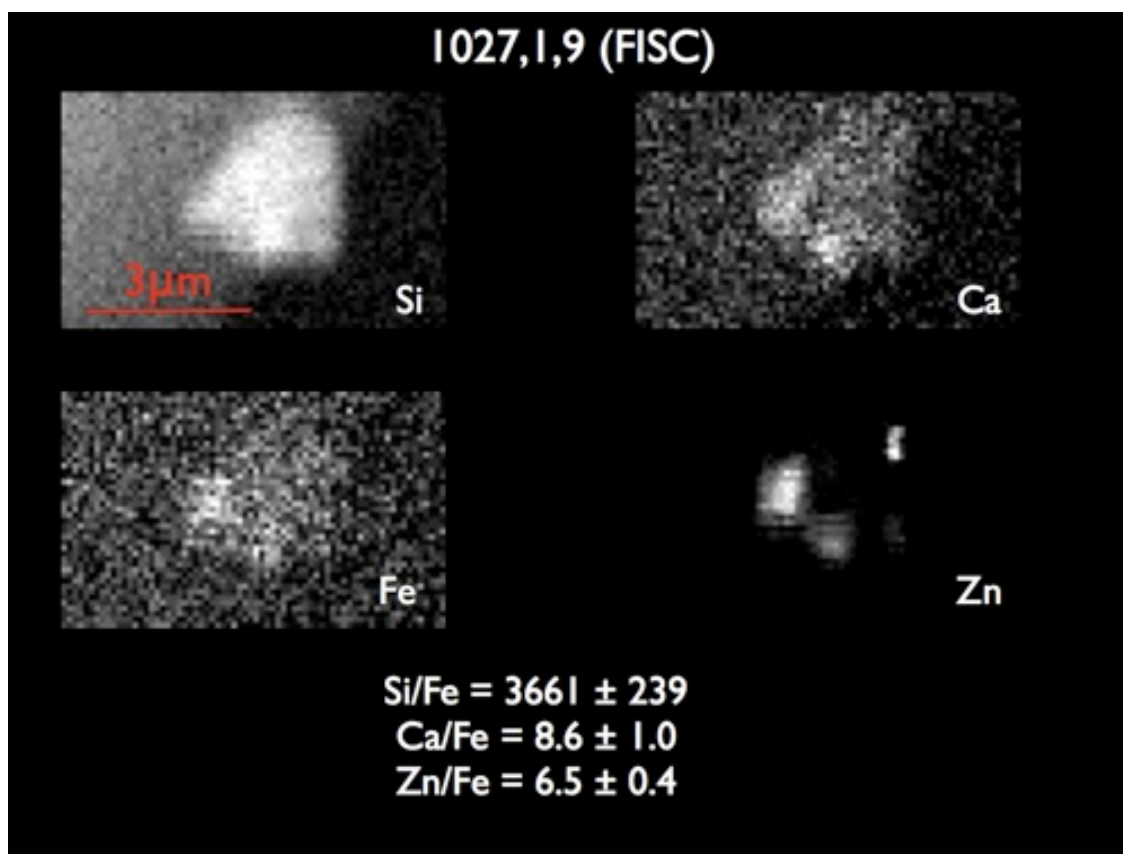


FIGURE 5. XRF maps of the first interstellar candidate, taken on ID22NI at the ESRF. The Ca/Fe, and Zn/Fe ratios are all significantly enhanced over CI values, indicating that it is unlikely to be of extraterrestrial origin.

XRF ANALYSIS OF CANDIDATES

Interstellar dust candidates have been analyzed at three X-ray fluorescence microprobes: ESRF ID13 and ID22NI at the European Synchrotron Radiation Facility and beamline 2-ID-D at the Advanced Photon Source, Argonne National Laboratory. Synchrotron X-ray fluorescence is sensitive to major, minor, and trace elements with $Z \geq 12$. Samples at the ESRF were analyzed with a focussed X-ray beam of 15.3 keV (ID13) and 17 keV (ID22NI), and at the APS with a 10 keV beam. All samples were successfully analyzed with a spatial resolution of ≤ 250 nm. Some off-normal candidates, like the one shown in Figure 4, were found to be rich in Ce, Zn, and Mg, consistent with the Ce-rich glass covers of the aft solar panels of the Stardust spacecraft. In these cases an interplanetary dust particle impact into the rear solar panels is likely to have produced debris that impacted the interstellar collector. In most cases, IS candidates were identified as probable terrestrial contaminants because of elemental ratios of, e.g. high Zn/Fe and Se/Fe. An example is shown in Figure 5. No detectable elements were found in a crater-like feature,

raising the possibility of a purely organic or other highly volatile impactor; however, no evidence of organic material was found by FTIR in this feature. The terminal particle in I1004,1,2 (shown in Figure 6) was found to have Cr/Fe, Mn/Fe, and Ni/Fe ratios significantly higher than CI, which is not the expected pattern for average interstellar dust because all four elements are believed to be almost fully condensed in the interstellar medium. However, this composition does not match any Stardust spacecraft component yet identified. Interstellar Candidate I1075,1,25 (shown in Figure 7) poses a similar problem. Four Fe-rich hot-spots were identified along an almost straight line, with an additional deposit of material at the exposed aerogel surface. Addition of the spectra from the surface feature and the four particles gives a Ni/Fe ratio consistent with CI. This Ni/Fe ratio is quite distinct from that of most natural terrestrial materials, and is frequently used to distinguish terrestrial from extraterrestrial particles. However, other refractory elements, including Ti, V, and Cr, are significantly enriched, as are several moderately-volatile elements, e.g., Cu, and Zn. The origin of the particles in I1004,1,2 and I1075,1,25 remains under investigation. In Table 2 we

TABLE 1. Photon fluence for mapping of several elements at ALS 11.0.2 STXM.

Edge	Map Energy (eV)	Photon Fluence (cm ⁻²)	attenuation length	
			20 mg/cm ³ aerogel (μm)	3.5 g/cm ³ olivine (μm)
C-K	280, 290	N/A	30	0.2
N-K	398, 406	N/A	60	0.4
Ti-K	450, 453	5.6×10 ¹⁴	80	0.6
O-K	525, 540	8.1×10 ¹⁴	120	0.8
Fe-L3	702, 708	9.4×10 ¹⁴	70	0.5
Ce-M5	875, 882	2.0×10 ¹⁵	120	0.8
Mg-K	1304, 1314	1.3×10 ¹⁵	320	0.9
Al-K	1560, 1570	2.9×10 ¹⁵	530	1.8
Si-K	1825, 1845	1.9×10 ¹⁵	250	1.5

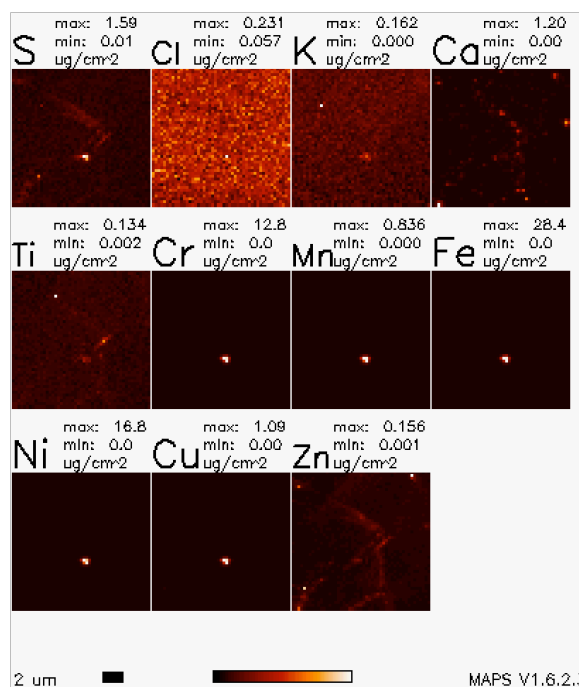


FIGURE 6. XRF maps of terminal particle in track I1004,1,2 taken on 2-ID-D at the APS. The Cr/Fe, Mn/Fe, Ni/Fe, and Cu/Fe ratios in this terminal particle are significantly enriched relative to cosmic abundances, and S/Fe, Ca/Fe, and Ti/Fe are all significantly below cosmic abundances.

summarize the analyses obtained so far on 14 interstellar dust candidates. We have not included the results from the FTIR beamlines in the table: so far no evidence of extraterrestrial organic material has been found in any of the candidates. Analyses of other tracks are in progress.

STXM ANALYSIS OF CANDIDATES

Candidates have been analyzed by Scanning Transmission X-ray Microscopy (STXM) at Beamline 11.0.2 at the Advanced Light Source at Lawrence Berkeley National Laboratory. The new generation STXM at ALS Beamline 11.0.2 has an elliptically polarized undulator (EPU) soft X-ray source, providing an energy range from 130 to 2000 eV. The synchrotron beam is focused to ~30 nm beam spot using Fresnel zone plates and the resolving power ($E/\Delta E$) is 2500-7000 (~80 meV at C K-edge). Every element with an edge in the instrument's extended energy range is accessible, only limited in this application by attenuation of X-rays by the 50 – 70 μm thickness of 20 mg/cm³ SiO₂ aerogel: elements with edges <400 eV, including C, N, Ca, and K, require greater flux. Table 1 shows the attenuation distances of X-rays at energies of some major elements in aerogel and, for comparison, olivine. Oxygen detection is limited by the aerogel background. Surprisingly, Si-mapping of silicates is quite effective in 70 μm thick aerogel. The sensitivity is in the fg mass range for most elements. As an example, using a combination of X-ray absorption mapping and XANES, we found the terminal particle of I1007,1,4,0,0 to be a 0.7 μm² diameter glass containing these metals (atom%): 36% Al, 21% Ce, 18% Na, 17% Zn, 8% Mg; oxygen was present but not quantified. An oxide glass was deduced from the Al X-ray Absorption Near Edge Structure (XANES) spectroscopy. We have also identified alumina in a candidate using Al-XANES. We have demonstrated that STXM can be used to image the track itself in the aerogel even in the absence of any residue of the projectile along the track (Figure 8). We have used the narrow focal depth (~5 μm at the Fe L-edge) to distinguish particles lying on the aerogel surface, not within a track, which highlights the need for these complementary techniques.

I1075,1,25: IS Candidate

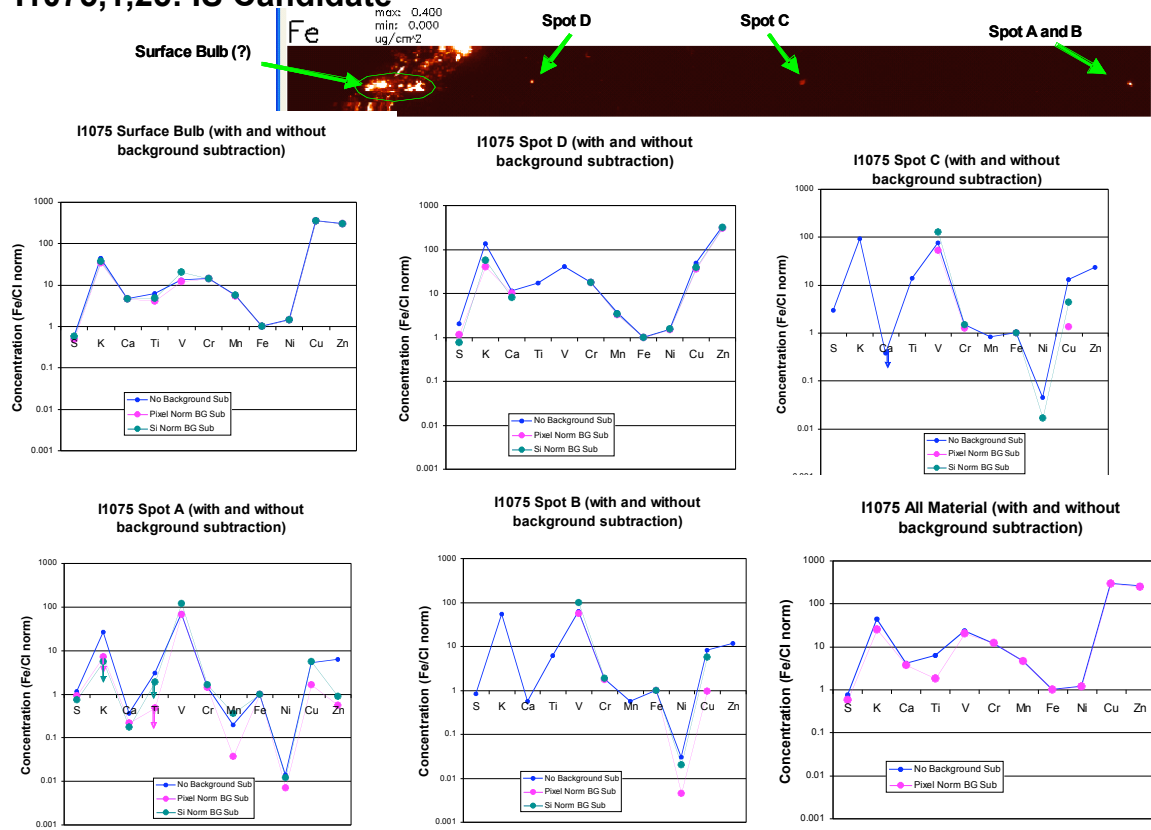


FIGURE 7. XRF maps of a region of interstellar dust candidate I1075,1,25,0,0 taken on 2-ID-D at the APS. The high-resolution map identified a possible entry hole or small bulb at the surface, which is most easily visible in the Al, Cr, and Fe images, and four Fe hot-spots (Spots A, B, C and D). The four Fe hot-spots are distributed along an almost straight line that points back to the linear feature at the surface. This has all the characteristics of an entry track, except that no track is visible in the optical microscope. Elemental compositions of the five individual features as well as the composition of the sum of all five features are compared to CI.

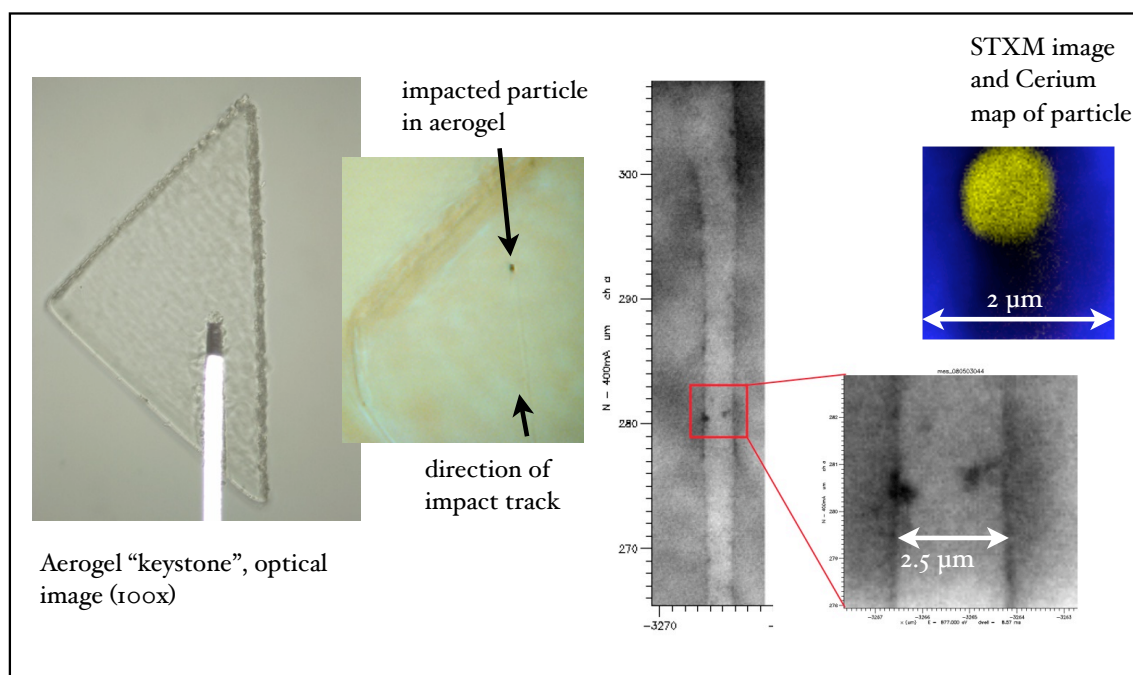


FIGURE 8. Absorption images (877 eV) of a portion of track I1017,2 in aerogel, taken on the STXM beamline 11.0.2 at the ALS.

CONCLUSION

The capabilities of the synchrotron microprobes involved in the search for interstellar dust captured in aerogel are well-matched to the extremely challenging nature of these samples. The first tracks extracted from the Stardust Interstellar Collector were selected because their orientations suggested they were likely to be spacecraft debris, which made them suitable for demonstrating the reliability of the extraction, mounting, and analytical techniques on material from the flight tray. Synchrotron measurements indicated that several of these particles had compositional similarities to spacecraft components, demonstrating that non-destructive synchrotron analysis techniques characterized these particles sufficiently well to eliminate them as possible interstellar grains. Among the subsequent extractions several particles have been identified with compositions that are not similar to any known spacecraft components. In each case the particle composition differs from the average composition of interstellar grains, inferred from astronomical measurements. The identification of rare interstellar/circumstellar grains of diverse compositions (graphite, silicon carbide, titanium carbide, corundum, spinel, hibonite, olivine etc.) in primitive meteorites demonstrates that interstellar grains exhibit a wide diversity of compositions, so further investigation of those grains whose compositions are not similar

to spacecraft components is in progress.

ACKNOWLEDGMENTS

This work was supported at UCB by a NASA DDAP grant, at Chicago through NASA grants NNX07-AL94G and NNX09-AG39G, and at SUNY-Plattsburgh through DDAP grant NNG06GG13G. The Advanced Light Source is supported by the Director, Office of Science, Office of Basic Energy Sciences, of the U.S. Department of Energy under Contract No. DE-AC02-05CH11231. Portions of this work were performed at the National Synchrotron Light Source (NSLS), Brookhaven National Laboratory. Use of the NSLS was supported by DOE under Contract No. DE-AC02-98CH10886. Use of the Advanced Photon Source was supported by the U. S. Department of Energy, Office of Science, Office of Basic Energy Sciences, under Contract No. DE-AC02-06CH11357. A.S., L.L. and T.F. acknowledge support from the French Centre National d'Etudes Spatiales (CNES).

TABLE 2. Summary of analyses of samples extracted from the interstellar tray. The interstellar candidates start with sample 9, although sample 2 is now considered to be a possible interstellar candidate. The beamlines are: ID13 and ID22NI are fluorescence X-ray microprobes at ESRF; 2-ID-D is a fluorescence X-ray microprobe at the APS; 11.0.2 is a Scanning Transmission X-ray Microscope at the ALS. Tracks 1, and 3-5 have orientations consistent with a secondary origin on the spacecraft. Tracks 7, 8 and 22 were lost before analysis.

Sample	Beamline(s)	Analysis	prob. of ET origin
1	ID13	Ce/Fe, Zn/Fe \gg CI	low
2	2-ID-D	Ni/Fe \sim CI, V/Fe, Cr/Fe, Zn/Fe $>$ CI	uncertain
3	11.0.2	Ce/Fe \gg CI	low
4	11.0.2	Ce/Fe \gg CI	low
5	ID22NI	off-normal trajectory	low
6	11.0.2	no detectable elements	uncertain
9	ID22NI	Zn/Fe = $\sim 4000 \times$ CI	low
10	11.0.2	no detectable elements	uncertain
11	11.0.2	alumina, surface feature	low
12	ID22NI	linear; S, Ni, no Fe	low
13	ID22NI	Ni, Cu, Zn, Sr/Fe gg CI	low
14	ID22NI	Ni, Cu/Fe \gg CI	low
15	ID22NI	Ni, Zn, Sr/Fe \gg CI	low
16	2-ID-D	Fe/Ni \sim CI; Cl, Cr, Cu/Fe \gg CI	low
17	2-ID-D	damaged; 3 spots analyzed: 1: K, Ti, Zn/Fe \gg CI 2 & 3: Cr, Mn, Ni/Fe $<$ CI	uncertain
18	11.0.2	no targets identified	uncertain
19	11.0.2	Surface feature; Si XANES looks like glass	low
20	ID13	Ni/Fe \sim CI, Cr, Mn/Fe \gg CI	low
	11.0.2	no detectable Mg, trace Al	
21	ID13	$50 \times 20 \mu\text{m}$ surface spider-like feature; K, Cu, Zn, Ge/Fe \gg CI	low
23	11.0.2	surface feature, Si, Al, Na present	low
24	11.0.2	possible high-angle track	uncertain
25	2-ID-D	V/Fe, Cu/Fe, Zn/Fe \gg CI	uncertain

REFERENCES

1. Tsou P. *et al.* J. Geophys. Res. E **109**, E12, CitelID E12S01 (2004)
2. Flynn G. J. *et al.* Science **314**, 1731 (2006)
3. Sandford S. A. *et al.* Science **314**, 1720 (2006)
4. Zolensky, M. E. *et al.* Science **314**, 1735 (2006)
5. Westphal A. J. *et al.* Astrophys. J. **694**, 18 (2009)
6. Bajt, S. *et al.* Meteoritics Planet. Sci. **44**, 471 (2009)
7. Baguhl, M. *et al.* Space Science Reviews, **72**, 471 (1995)
8. Savage, B. D. and Sembach K. R., Astrophys. J. **475**, 211 (2009)
9. Zhukovska, S. *et al.* A&A 479, 453 (2008)
10. Burchell M. *et al.* Meteoritics Planet. Sci. **43**, 23 (2008)
11. Westphal A. J. *et al.* Meteoritics Planet. Sci., **39**, 1375 (2004)